Title	Coupling Serpent and OpenFOAM for neutronics - CFD multi-physics calculations
Citation	Proceedings of PHYSOR 2016, May 1 - 5 May 2016
Rights	This is a post-print version of the article and it may be downloaded for personal use.

COUPLING SERPENT AND OPENFOAM FOR NEUTRONICS – CFD MULTI-PHYSICS CALCULATIONS

R. Tuominen, V. Valtavirta, J. Peltola, and J. Leppänen
VTT Technical Research Centre of Finland Ltd
riku.tuominen@vtt.fi

ABSTRACT

The main goal of this work was to couple the Monte Carlo neutronics code Serpent 2 with a CFD solver from the OpenFOAM toolbox. The coupling was implemented with the already available multi-physics interface of Serpent. The interface allows the passing of high fidelity density and temperature distributions from an external solver to Serpent and also the passing of fission power distribution from Serpent to the external solver. The coupled CFD-neutronics problem was solved by iteration.

The coupling was tested by modelling a mock-up 5x5 fuel assembly cooled with water in a steady state condition at full power. The effects of boiling were neglected and the flow was modelled as single phase. The main results of the coupled calculation were high fidelity temperature and density distributions. The effect of distribution fidelity on neutronics was studied by running Serpent simulations with varying level of axial refinement. Most obvious differences were observed in the axial power density and in the collision density in the coolant, with minor differences in e.g. the effective multiplication factor.

In addition the convergence of the coupled calculation was briefly studied. The default Serpent relaxation scheme based on the stochastic approximation performed well in the coupled calculations. This work can be continued in the future for example by including the effects of boiling in the CFD solution.

Key Words: **Monte Carlo neutronics, CFD, multiphysics**

1. INTRODUCTION

Accurate modelling of a nuclear reactor is a non-trivial task. It is not enough to only consider the neutronics of the core as several important feedback mechanisms exist. One of the most important ones is related to thermal-hydraulics as the temperature and density distributions of different materials have a major effect on the neutron flux distribution. An increase in the moderator temperature results in a decrease in moderator density and moderating effectiveness. This in turn hardens the neutron spectrum which gives rise to negative reactivity addition in a thermal reactor. In the fuel the neutron flux is mainly affected by the Doppler broadening of the effective resonance cross sections. As the fuel temperature increases so does the resonance absorption of neutrons.

The availability of relatively cheap, high speed parallel computers has triggered a growing interest in the development of high-fidelity reactor simulation tools. These are intended to provide reference solutions for the less accurate methods used currently and perhaps replace the current methods in the modelling of small-scale systems. One of the major goals is to increase the spatial resolution of the solution.

The goal of this work was to develop an external coupling between the Monte Carlo neutronics code Serpent 2 and computational fluid dynamics (CFD) solver from the open source OpenFOAM toolbox. For simplicity, only a steady state case with single phase flow was considered. The coupled problem was solved by iteration. To test the coupling a mock-up 5x5 fuel assembly was modelled. The results of this calculation were high fidelity temperature and density distributions which were used as an input for a separate Monte Carlo simulation. In addition several simulations were run with less accurate distributions to find out how the spatial fidelity of the temperature and density distributions affects neutronics. The convergence of the coupled calculation was also briefly studied.

2. METHODS

2.1. Serpent

Serpent [1] is a state-of-the-art Monte Carlo reactor physics code developed at VTT Technical Research Centre of Finland since 2004. The code was originally written for spatial homogenization but has gained many additional features over the years of development. These include built-in burnup calculation capability and a multi-physics interface which allows coupling to external CFD, thermal hydraulics and fuel performance codes [2]. Serpent uses several special methods for efficient simulation of the neutrons. These include Woodcock delta tracking for neutron transport which simplifies the geometry routine and reduces calculation times, and on-the-fly temperature treatment routine based on the Target Motion Sampling (TMS) technique [3] which reduces significantly the required cross section data to store in RAM memory.

The multi-physics interface allows modelling of materials with arbitrarily refined temperature and density distributions supplied by an external solver. The coupling is implemented by separating the state point information (temperature and density) from the Monte Carlo geometry routine. This is made possible by using rejection sampling for neutron path lengths and on-the-fly TMS temperature treatment for microscopic cross sections. One format to pass the temperature and density distributions is based on the OpenFOAM unstructured mesh format [4].

The mesh based interface features a separate superimposed search mesh to speed up the cell search for finding correct state point information at each interaction point. The size of the search mesh has a considerable effect on both memory usage and required calculation time. Implementing a coupling with the mesh based interface is easy since the interface allows the passing of density and temperature distributions without modification from the CFD solver to Serpent but in addition, it makes it possible to pass a power distribution back from Serpent to the CFD-solver tallied directly on the mesh used by the CFD-solver. It is also possible to define the problem geometry based on the OpenFOAM mesh which enables modelling of complex irregular geometries [5].

2.2. OpenFOAM

OpenFOAM (Open Field Operation And Manipulation) [6] is a free, open source C++ toolbox for continuum mechanics problems, including CFD distributed by the OpenFOAM Foundation. It can be used to solve an extensive range of problems from complex fluid flows involving chemical reactions, turbulence and heat transfer, to electrodynamics and solid dynamics. OpenFOAM version 2.3.1 was used in this work.

The base of OpenFOAM is a large library which offers the core functionality of the code such as tensor and field operations, discretization of partial differential equations, mesh, solution to linear equations, turbulence models etc. By using this library the user can develop applications such as solvers for partial differential equations or extensions such as new boundary conditions. OpenFOAM also includes over 80 ready made solvers, each for a specific problem, and tools for meshing and pre- and post-processing. Almost everything in OpenFOAM runs in parallel.

3. COUPLING

A simple coupling program was used in order to automatically run Serpent and OpenFOAM in turns. The iteration is started by running a Serpent simulation with uniform material-wise temperature and density distributions. The resulting fission heat source is passed to the OpenFOAM solver which calculates new temperature and density distributions. Next step is to continue the Monte Carlo simulation with the updated distributions. A fixed number of active neutron histories is simulated in Serpent on each iteration. The iteration cycle is continued until user-defined maximum number of iterations is reached. All information between Serpent and the OpenFOAM solver is transferred using OpenFOAM field files.

At each iteration the convergence of the individual OpenFOAM calculation is determined by monitoring energy balance in the fluid. The balance is calculated by integrating the convective and diffusive fluxes of enthalpy over the fluid region boundaries

$$B = \int_S \rho h \vec{U} \cdot \vec{n} \mathrm{d}S + \int_S \alpha \nabla h \cdot \vec{n} \mathrm{d}S,$$

where ρ, h, $\vec{U}$ and α are the density, specific enthalpy, velocity and thermal diffusivity, respectively.

In a steady flow the balance should be equal to zero as the enthalpy (or temperature) field is constant in time and there are no heat sources in the fluid region. The actual variable monitored by the OpenFOAM solver describes relative energy balance and it is calculated by dividing the absolute value of the energy balance with enthalpy flux from the regular fuel rods

$$B_{\text{rel}} = \frac{|B|}{\int_{S_{\text{f}}} \alpha \nabla h \cdot \vec{n} \mathrm{d}S}.$$

The iteration is stopped when the relative energy balance has been lower than an user specified limit for an user specified number of time steps in a row.

The stochastic nature of the Monte Carlo neutronics poses a significant convergence challenge in the coupled calculations. There is always some statistical uncertainty in the fission power distribution. To overcome this problem Serpent uses a relaxation scheme based on the stochastic approximation scheme presented in Reference [7]. The fission power distribution is relaxed according to

$$P_{\text{rel}}^{(n+1)} = P_{\text{rel}}^{(n)} - \frac{s_{n+1}}{\sum\limits_{i=1}^{n+1} s_i} \alpha (P_{\text{rel}}^{(n)} - P^{(n+1)}),$$

where $P_{\text{rel}}^{(n+1)}$ and $P_{\text{rel}}^{(n)}$ are the relaxed power distributions on iterations $n+1$ and n. $P^{(n+1)}$ is the iteration-wise power distribution on iteration $n+1$, s_i is the number of simulated neutrons on iteration i and α is an additional under-relaxation factor. It can be shown easily with mathematical induction that this relaxation scheme combines the power distributions of all of the iterations with weights $s_i / \sum_i s_i$. If the same number of neutron histories is simulated on each iteration, the weight simplifies to $1/n$, where n is the number of iterations. With each iteration the statistical uncertainty in the power distribution is reduced and by running enough iterations any convergence level can be reached.

To demonstrate the effectiveness of the stochastic approximation based relaxation scheme an additional coupled calculation was run with a fixed under-relaxation factor. The power distribution was relaxed on each iteration according to

$$P_{\text{rel}}^{(n+1)} = (1 - \alpha) P_{\text{rel}}^{(n)} + \alpha P^{(n+1)},$$

where the under-relaxation factor α was set to $\alpha = 0.1$.

4. TEST CASE

The Serpent-OpenFOAM coupling was tested with a case based on PWR TMI-1 assembly presented in OECD benchmarks [8] and [9]. The test case models a mock-up 5x5 fuel assembly cooled with water in a steady state condition at full power. Reflective boundary conditions are used horizontally so the test case is horizontally infinite. Axially the problem is finite. The following sections describe the test case geometry, materials and other parameters, and also how the case was modelled with Serpent and OpenFOAM.

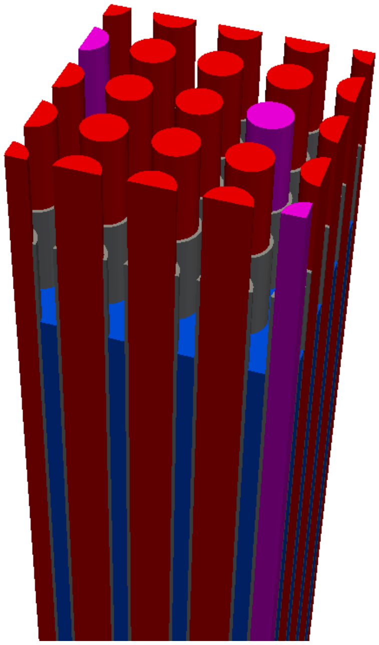

Figure 1. 3D-render of the test case geometry with the following colours: regular fuel in red, gadolinia fuel in purple, cladding in grey and coolant in blue.

Table I. Fuel assembly design parameters for the test case

Parameter	Value
Fuel assembly dimensions	5x5
Fuel rod length (mm)	3600
Unit cell pitch (mm)	14.427
Fuel pellet diameter (mm)	9.391
Regular fuel material	UO_2
Regular fuel density (g/cm^3)	10.283
Regular fuel enrichment (w/o)	4.85
Gadolinia fuel material	UO_2+Gd_2O_3
Gadolinia fuel density (g/cm^3)	10.144
Gadolinia fuel enrichment (w/o)	4.12
Gd_2O_3 concentration (wt. %)	2.0
Cladding material	Zircaloy-4
Cladding density (g/cm^3)	6.55
Cladding outside diameter (mm)	10.928
Cladding thickness (mm)	0.673

4.1. Geometry and Materials

3D-render of the modelled 5x5 assembly is shown in Figure 1 and the design parameters are presented in Table I. The assembly contains both regular UO_2 fuel pins and gadolinia fuel pins with integral Gd burnable poison. The cladding in all of the fuel rods is Zircaloy-4 with the following composition presented in weight percent: O 0.125 %, Cr 0.100 %, Fe 0.210 %, Zr 98.115 % and Sn 1.450 %. The gap between cladding and fuel is modelled differently in OpenFOAM and Serpent.

4.2. OpenFOAM Model

The CFD calculations were performed with a slightly modified version of the chtMultiRegionSimpleFoam solver which is designed for conjugated heat transfer (CHT) problems with buoyant, turbulent flows of compressible fluids including radiation. The ”Multi-Region” in the name of the solver refers to the fact that each subdomain or region has its own mesh. The Navier-Stokes equations are solved with SIMPLE algorithm.

In the OpenFOAM model the test case geometry is divided into four regions, three of which are solid regions and one is a fluid region. The first region contains the water flowing past the fuel rods, second the cladding of all fuel rods, third the regular fuel and fourth the fuel with gadolinia. The gap between a fuel pellet and cladding is not included in the geometry and it is replaced with cladding. The effect of the gap is taken into account by introducing a thermal resistance between the fuel and the cladding with a boundary condition. Meshes were generated with *snappyHexMesh* application included in the OpenFOAM distribution. The total number of cells is 2228224 with the following distribution: fluid 1175040, cladding 589824, regular fuel 412672 and gadolinia fuel 50688.

The fluid flow was modelled as compressible and the thermophysical properties of water were evaluated with libFluid which is a thermophysical library developed at VTT. Turbulence was modelled with k-ω SST turbulence model and near wall treatment was implemented with wall functions. For the velocity Spalding continuous law-of-the-wall wall function [10] was used and for heat tranfer the Jaytilleke [11] correction were applied. In the k-ω SST model blended near-wall ω formulation by Menter [12] was applied.

Boundary conditions were the following. $symmetry$ boundary condition was used horizontally at the boundaries of the computational domain to model a horizontally infinite problem. At the inlet of the fluid region *mapped* boundary condition was used for the velocity to create a periodic flow. The velocity profile was sampled at a distance of $8\,\mathrm{cm}$ from the inlet and scaled to an average value of $3.6\,\mathrm{m/s}$. Temperature at the inlet was fixed to a value of $561\,\mathrm{K}$. Pressure at the outlet was set to a fixed average value of $15.51\,\mathrm{MPa}$. Modified version of *turbulentTemperatureCoupledBaffleMixed* was used to connect different material regions. The boundary conditions balances heat flux calculated using enthalpy on the boundary.

The densities of the both fuel types and the cladding were constant in the calculations, and they are presented in Table I. To evaluate thermophysical properties of the both fuel types and the cladding a couple of new thermophysical submodels were created. The specific heat and the thermal conductivity of the fuel are given by FRAPTRAN correlation presented in Reference [13]. For the cladding it was necessary to create only one new submodel which evaluates specific heat capacity and enthalpy. The thermal conductivity is evaluated with ready made *polynomialTransport* submodel which calculates the thermal conductivity from a polynomial with constants specified by FRAPTRAN correlation [13]. The specific heat capacity of the cladding is calculated by linear interpolation from values presented in Reference [13] for Zircaloy alloys.

Thermal resistance was added to the fuel-cladding interface using a boundary condition to model the effect of the gas gap. The values specifying the thermal resistance were $\kappa = 0.2731\,\mathrm{W/(m \cdot K)}$ and $\Delta = 3.55 \times 10^{-5}\,\mathrm{m}$ which are the thermal conductance and thickness of the artificial layer inducing the thermal resistance.

4.3. Serpent Model

In the coupled calculations the problem geometry in Serpent was defined with Serpent's own CSG-based geometry model. It's also possible to generate the geometry based on the unstructured OpenFOAM mesh or meshes but this can slow down the neutron-tracking in a case, where the normal CSG-based geometry is simple. The gas gap between the cladding and the fuel pellet was modelled as void. In the x- and y-directions reflective boundary condition and in the z-direction black boundary condition was used to model a horizontally infinite problem.

The k-eigenvalue criticality source method was used in the Serpent calculations. At each iteration of the coupling program 40 million active neutron histories divided into 100 cycles of $400\,000$ source neutrons were simulated. In addition on the first iteration 50 inactive cycles were run before starting to collect the results in order to allow the initial fission source distribution to converge. On the following iterations the number of inactive cycles was reduced to 20. The power distribution was relaxed on each iteration with a relaxation scheme presented in Section 3.

The iteration process was started by running a Serpent calculation with uniform temperature and density distributions which produced a cosine shaped power distribution peaking at the center of the assembly. To accelerate convergence this initial power distribution was disregarded in the calculation of the relaxed power distribution on the sequential iterations. Total heating power was set to $1.0368\,\mathrm{MW}$.

5. RESULTS

5.1. Coupled Calculation

The coupled calculation was run for 60+1 iterations. The total calculation time was approximately $72\,\mathrm{h}$ on a computer node consisting of two Eight-Core Intel Xeon E5-2680 $2.7\,\mathrm{GHz}$ processors with $128\,\mathrm{GB}$ RAM memory. The OpenFOAM solver utilized 16 processors with OpenMPI library and Serpent was run with 16 OpenMP threads. The main results of this calculation are the high fidelity temperature and density distributions which can be used in an independent Monte Carlo simulation.

Axial temperature distributions are presented in Figure 2 and horizontal temperature distributions in Figure 3. The fuel and the cladding temperature distributions are presented on a plane with a normal parallel with y-axis and origin at $y \approx -0.028\,\mathrm{m}$. The plane intercepts approximately the center of each fuel rod in the bottom row. The axial temperature distribution of the coolant is presented on a plane with a normal parallel with the y-axis and origin at $y \approx -0.022\,\mathrm{m}$. The plane is located at the middle of the coolant region between the two bottommost fuel rod rows. The horizontal distributions are presented on plane with a normal parallel with z-axis and origin at $z \approx -0.58\,\mathrm{m}$. The power density and therefore fuel temperature has its maximum approximately at this height.

The power density and fuel temperature peak at the lower half of the assembly with a maximum approximately at $z \approx -0.58\,\mathrm{m}$ due to moderation which is reduced as the coolant heats up while it flows through the assembly. The average coolant temperature at inlet is $T_{\text{inlet}} \approx 561\,\mathrm{K}$ and at outlet $T_{\text{outlet}} \approx 598\,\mathrm{K}$. There is a temperature jump in the fuel cladding interface due to the added thermal resistance in the OpenFOAM model.

Approximately 95 % of the total power is produced in the rods with regular fuel. This is expected as the gadolinium in the poisoned fuel absorbs effectively neutrons and suppresses the neutron flux. Due to the uneven power distribution in the regular and poisoned fuel, average temperature in the regular fuel is approximately 920 K and in the poisoned fuel 700 K. The effect of the uneven power distribution is also observed in the coolant temperature. Coolant temperature near the fuel rods with gadolinia is lower than in the other parts of the assembly.

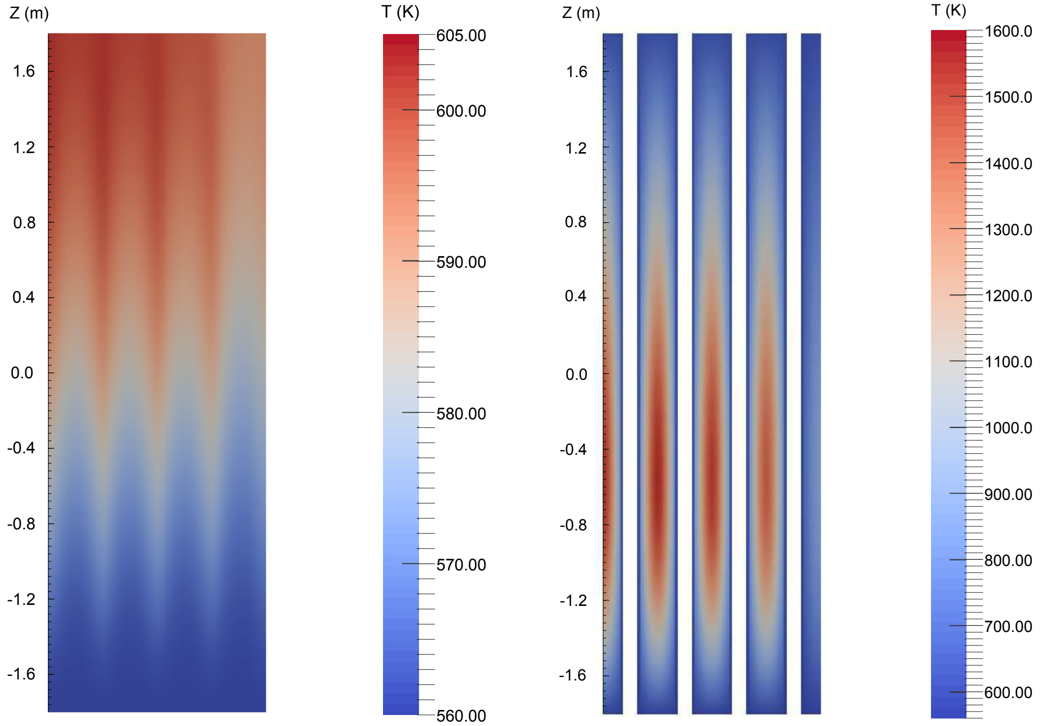

(a) Coolant

(b) Fuel and cladding

Figure 2. Axial temperature distributions at $y \approx -0.022\,\mathrm{m}$ for the coolant and at $y \approx -0.028\,\mathrm{m}$ for the fuel and the cladding.

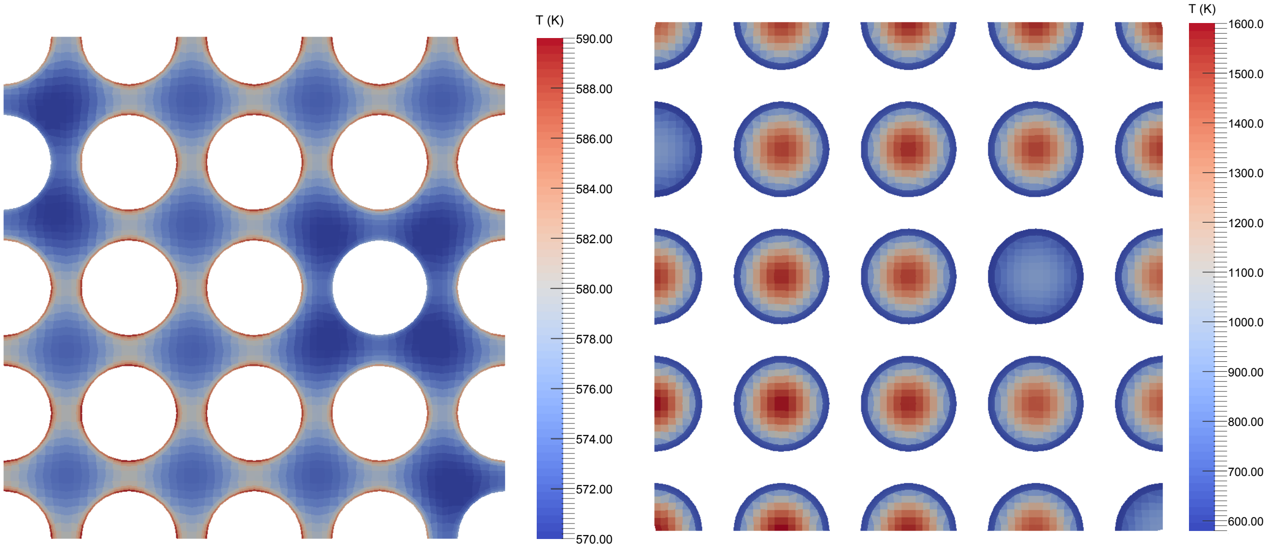

(a) Coolant

(b) Fuel and cladding

Figure 3. Horizontal temperature distributions at $z \approx -0.58\,\mathrm{m}$.

5.2. Effect of Spatial Fidelity on Results

The effect of temperature and density field fidelity on the Monte Carlo neutronics was tested by running an identical Serpent calculation multiple times, each time with different level of axial temperature and density field refinement. The assembly was divided axially into 1, 4, 8, 16 or 256 layers with uniform temperature and density distribution. 256 corresponds to the number of axial cell layers in the OpenFOAM mesh. 16 is close to the number of layers in typical nodal core simulators. In addition one run was performed with the reference temperature and density distributions obtained from the coupled calculation. Each layer-wise temperature value was calculated as cell volume weighted average of the reference cell temperatures in the specific layer. A separate value was calculated for each OpenFOAM region or material so that the regular fuel, the gadolinia fuel, the cladding and the coolant had separate temperature distributions. The fuel and the cladding had already uniform density in the model so no averaging was necessary. Layer wise density distribution in the coolant was calculated with libFluid from the layer-wise temperature distribution and average pressures. At each Serpent calculation one billion active neutron histories divided into 5000 cycles of $200\,000$ source neutrons were simulated. In addition 50 inactive cycles were run.

Table II presents the effective multiplication factor, mean neutron generation time, mean neutron lifetime and effective fraction of delayed neutrons for each level of axial refinement. No notable differences are observed in the mean neutron lifetime and in the delayed neutron fraction. The mean neutron generation time shows a difference between the calculation with constant material-wise distributions and the more refined cases. The effective multiplication factor increases as the level of axial refinement decreases. The biggest jump occurs from 4 axial layers to constant material-wise properties. It seems that a peaked temperature distribution and the corresponding density distributions has a larger negative reactivity effect than uniform distributions.

Table II. Effective multiplication factor $\mathrm{k_{eff}}$, mean neutron generation time Λ, mean neutron lifetime l and effective fraction of delayed neutrons β_{eff} for each level of axial refinement.

	$\mathrm{k_{eff}}$	Λ (s)	l (s)	β_{eff}
Reference	$1.166\,05 \pm 2 \times 10^{-5}$	$1.1995 \times 10^{-5} \pm 2 \times 10^{-9}$	$1.3986 \times 10^{-5} \pm 2 \times 10^{-9}$	$7.07 \times 10^{-3} \pm 1 \times 10^{-5}$
256	$1.166\,13 \pm 2 \times 10^{-5}$	$1.1993 \times 10^{-5} \pm 2 \times 10^{-9}$	$1.3984 \times 10^{-5} \pm 2 \times 10^{-9}$	$7.07 \times 10^{-3} \pm 1 \times 10^{-5}$
16	$1.166\,15 \pm 2 \times 10^{-5}$	$1.1996 \times 10^{-5} \pm 2 \times 10^{-9}$	$1.3989 \times 10^{-5} \pm 2 \times 10^{-9}$	$7.08 \times 10^{-3} \pm 1 \times 10^{-5}$
8	$1.166\,30 \pm 2 \times 10^{-5}$	$1.1993 \times 10^{-5} \pm 2 \times 10^{-9}$	$1.3988 \times 10^{-5} \pm 2 \times 10^{-9}$	$7.06 \times 10^{-3} \pm 1 \times 10^{-5}$
4	$1.166\,86 \pm 2 \times 10^{-5}$	$1.1992 \times 10^{-5} \pm 2 \times 10^{-9}$	$1.3992 \times 10^{-5} \pm 2 \times 10^{-9}$	$7.06 \times 10^{-3} \pm 1 \times 10^{-5}$
Constant	$1.168\,36 \pm 2 \times 10^{-5}$	$1.1970 \times 10^{-5} \pm 2 \times 10^{-9}$	$1.3985 \times 10^{-5} \pm 2 \times 10^{-9}$	$7.07 \times 10^{-3} \pm 1 \times 10^{-5}$

The normalized axial power distribution for each level of refinement is presented in Figure 4. Each distribution was formed by tallying the total fission energy production in 256 axial bins. The power distribution calculated with constant material-wise density and temperature distributions has a cosine like shape with a maximum in the middle of the assembly as expected. The other power distributions are closer to the reference. What is interesting, is the fact that there is an observable difference between the reference and the power distribution obtained with 256 axial layers. Both distributions peak at the same height but the one with 256 layers is shifted towards the upper half of the assembly. This indicates that

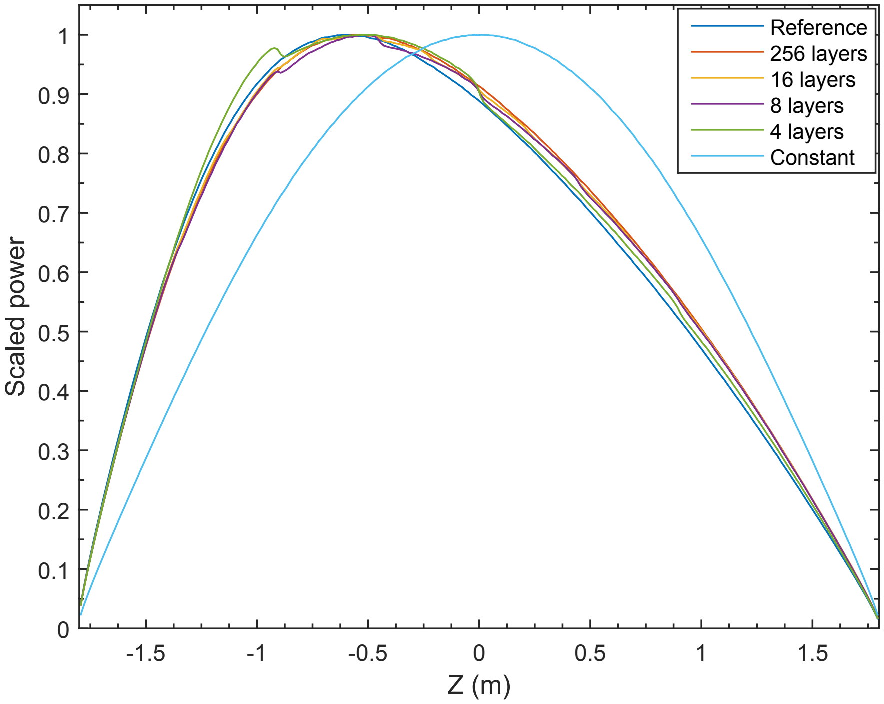

Figure 4. Normalized power distribution for each level of axial refinement.

the radial refinement which is lost in the averaging process has a large enough effect to be observable even in the axial power profile. Important variations in the horizontal temperature field result from the fact that certain fuel rods heat up more than others and these differences also affect the density distribution of the surrounding coolant. If spacer grids are added to the assembly, the differences are probably smaller as the grids increase mixing of the water.

Collision density in the moderator for the reference and for the run with 256 axial layers is presented in Figures 5(a) and 5(b). The collisions were tallied in 2500 bins with equal volumes with 50 bins in the x-direction ($x_{\mathrm{min}} = -0.028\,854\,\mathrm{m}$, $x_{\mathrm{max}} = -0.014\,427\,\mathrm{m}$), and 50 bins in the y-direction ($y_{\mathrm{min}} = 0.0\,\mathrm{m}$, $y_{\mathrm{max}} = 0.014\,427\,\mathrm{m}$). In the z-direction the bin limits were $z_{\mathrm{min}} = -0.6\,\mathrm{m}$ and $z_{\mathrm{max}} = -0.5\,\mathrm{m}$.

In both figures the collision density decreases near the rod in the upper left corner. This rod contains gadolinium which effectively absorbs neutrons resulting in a decrease in the neutron flux and collision density. In the reference case the decrease is slightly compensated by higher moderator density near the gadolinia rod compared to regular rods as less power is produced in the gadolinia fuel and therefore the surrounding water is in lower temperature. As the macroscopic total cross-section is directly proportional to density, higher moderator density leads to higher collision density. The non-uniform horizontal density distribution is also the reason why the collision density is elevated in the middle of the flow channel, where the water temperature is lower and density higher. These observations are limited to the reference case, as in the other cases the density distribution is horizontally uniform. The moderator density for the reference case at $z = -0.55\,\mathrm{m}$ is presented in Figure 6.

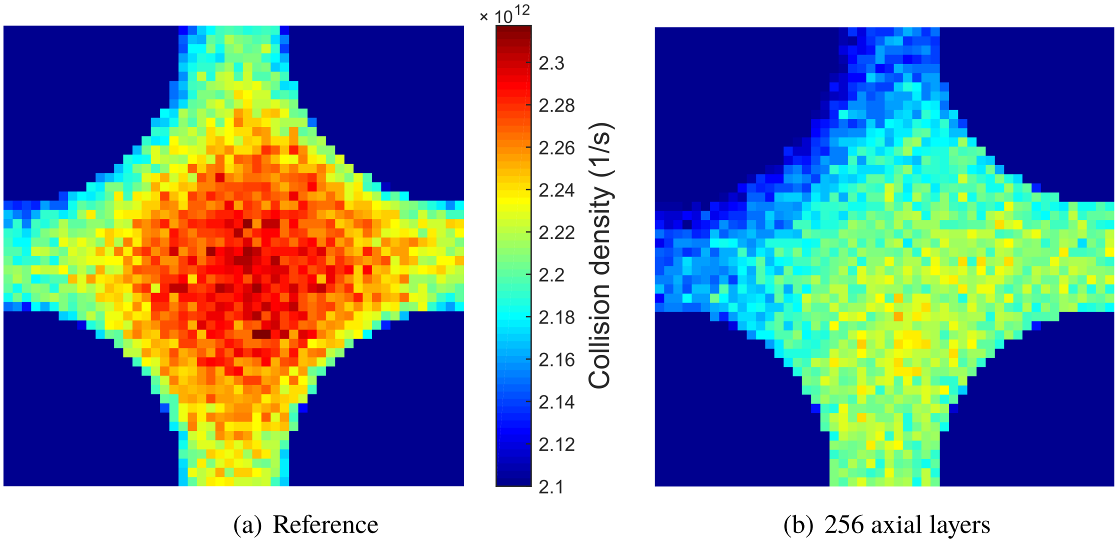

(a) Reference

(b) 256 axial layers

Figure 5. Collision density in the moderator.

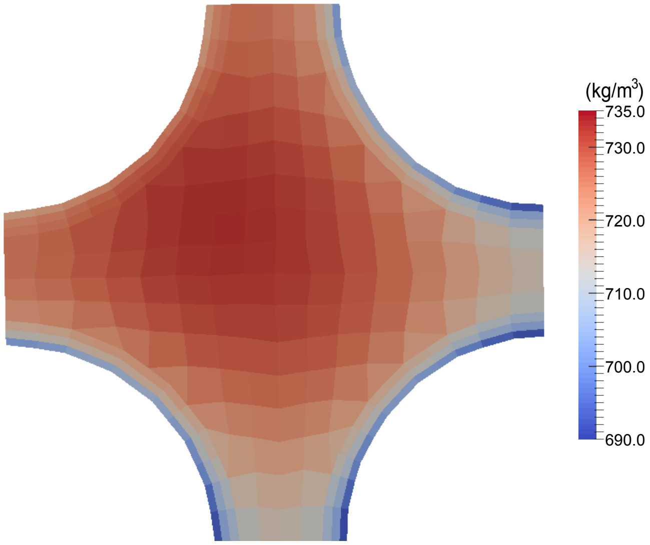

Figure 6. Moderator density for the reference distributions at $z = -0.55\,\mathrm{m}$.

5.3. Power Feedback Coefficient

Using the coupling it was possible to calculate a feedback coefficient for power. First, a coupled calculation was run with 5 % higher power to generate new temperature and density fields. Secondly, a

Monte Carlo simulation was run with these fields to get a new multiplication factor k_1. The resulting reactivity change was evaluated according to

$$\Delta\rho = \rho_1 - \rho_0 = \frac{k_1 - k_0}{k_1 k_0},$$

where k_0 is the effective multiplication factor from the simulation with unmodified distributions. The feedback coefficient is then calculated as

$$f = \frac{\Delta\rho}{\Delta\theta},$$

where $\Delta\theta$ is the difference in the power expressed also as percentage. An error estimate based on total differential is evaluated as

$$\epsilon_f = \frac{1}{\Delta\theta}\left(\frac{\epsilon_{k_0}}{k_0^2} + \frac{\epsilon_{k_1}}{k_1^2}\right),$$

where ϵ_{k_0} is the error in the original effective multiplication factor and ϵ_{k_1} is the error in the effective multiplication factor from the simulation with modified distributions. The feedback coefficient was f = $-27 \pm 2\,\mathrm{pcm}/\%$.

5.4. Relaxation and Convergence

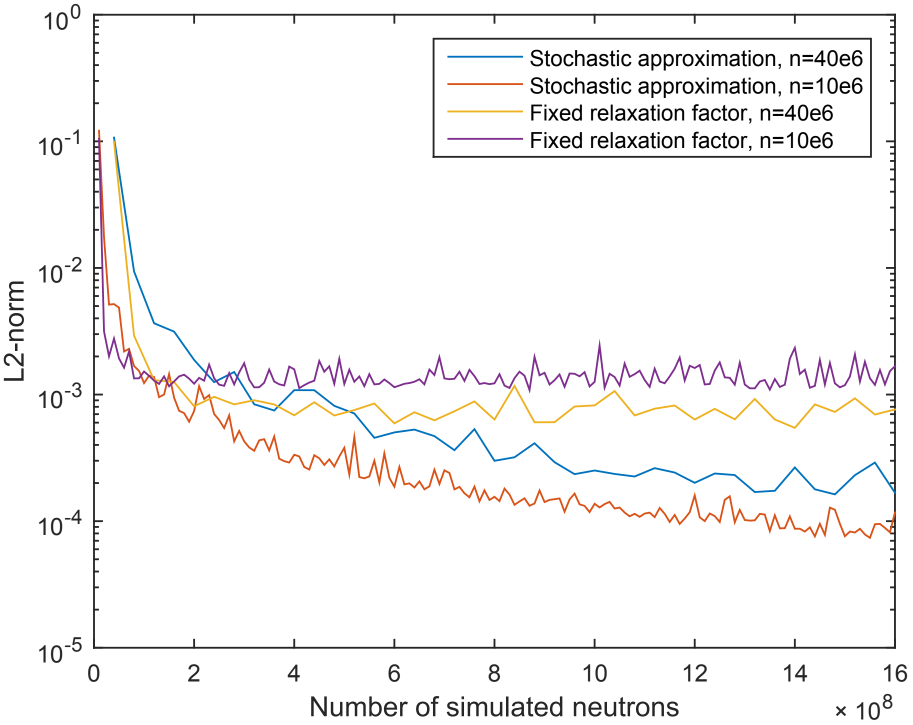

Figure 7. L2-norm of the fuel temperature for both tested relaxation schemes with two different number of simulated neutrons per iteration.

The convergence of the coupled calculation was evaluated retrospectively by comparing the regular fuel temperature distributions on two consecutive iterations. The variations in the regular fuel temperature from iteration to iteration were larger than in other regions as most of the fission heat was deposited in this fuel type. Volume weighted L2-norms of the relative difference in the fuel temperature for both tested relaxation schemes with two different number of simulated neutrons per iteration are presented in Figure 7. The L2-norm is defined as

$$E_{\mathrm{L2}} = \sqrt{\sum_i \frac{V_i}{V} \left(\frac{T_i^{(n+1)} - T_i^{n}}{T_i^{(n+1)}} \right)^2},$$

where V_i, $T_i^{(n+1)}$ and $T_i^{(n+1)}$ are the volume and the temperatures on iterations $n+1$ and n of the fuel cell with index i, respectively. V is the total volume of the fuel. With the fixed under-relaxation factor the convergence of the solution was limited by the uncertainty of the Monte Carlo simulation. This problem was not encountered with the stochastic approximation based relaxation, the performance of which was excellent and the uncertainty decreased roughly as $1/n$ as predicted by theory.

6. CONCLUSIONS

The main goal of this work was to implement an external coupling between Serpent and OpenFOAM CFD solver. The goal was achieved successfully with a simple coupling program and small modifications to the CFD solver. The coupling was tested by modelling a mock-up 5x5 assembly in a steady state with one phase flow. The main results of the coupled calculation were high fidelity temperature and density fields for separate Monte Carlo neutronics simulations. The effect of temperature and density distribution fidelity on the Monte Carlo results was tested by running a Serpent simulation multiple times with varying level of axial refinement. Differences were observed for example in the axial power distribution and the effective multiplication factor.

The models used in this work contain many limitations and there are many possibilities for future development. First of all, the CFD simulation should account for boiling and multiphase flow. Development of boiling modelling capability for OpenFOAM Eulerian multiphase CFD solvers is an on-going work topic at VTT in co-operation with OpenFOAM Foundation and CFD Direct Ltd.

Secondly the fuel behaviour could be modelled more accurately. In the current model only the temperature of the fuel is considered. Several separate fuel behaviour solvers exist so in the future OpenFOAM should only be used to solve the fluid flow to get more reliable results. This complicates the coupling as now three separate codes have to be coupled instead of only two.

Finally, the coupling scheme itself could be modified. The external file based coupling could be replaced with internal coupling based on direct memory access.

REFERENCES

[1] J. Leppänen et al. The Serpent Monte Carlo code: Status, development and applications in 2013. *Ann. Nucl. Energy.*, 82:142–150, 2015.

[2] J. Leppänen et al. The Numerical Multi-Physics project (NUMPS) at VTT Technical Research Centre of Finland. *Ann. Nucl. Energy.*, 84:55–62, 2015.

[3] T. Viitanen. Development of a stochastic temperature treatment technique for Monte Carlo neutron tracking. D.Sc. Thesis, Aalto University, 2015. (VTT Science 84).

[4] J. Leppänen et al. Unstructured Mesh Based Multi-Physics Interface for CFD Code Coupling in the Serpent 2 Monte Carlo Code. In proc. PHYSOR 2014, Kyoto, Japan, Sep. 28 - Oct. 3, 2014.

[5] J. Leppänen and M. Aufiero. Development of an Unstructured Mesh Based Geometry Model in the Serpent 2 Monte Carlo Code. In proc. PHYSOR 2014, Kyoto, Japan, Sep. 28 - Oct. 3, 2014.

[6] OpenFOAM Foundation. OpenFOAM. http://www.openfoam.org. (15.12.2015).

[7] J. Dufek and W. Gudowski. Stochastic approximation for Monte Carlo calculation of steady-state conditions in thermal reactors. *Nuclear science and engineering*, 152(3):274–283, 2006.

[8] K. Ivanov et al. Benchmarks for Uncertainty Analysis in Modelling (UAM) for the Design, Operation and Safety Analysis of LWRs-Volume I: Specification and Support Data for Neutronics Cases (Phase I). Technical report, Organisation for Economic Co-Operation and Development, Nuclear Energy Agency-OECD/NEA, Le Seine Saint-Germain, 12 boulevard des Iles, F-92130 Issy-les-Moulineaux (France), 2013.

[9] T. Blyth et al. Benchmarks for Uncertainty Analysis in Modelling (UAM) for the Design, Operation and Safety Analysis of LWRs-Volume II: Specification and Support Data for the Core Cases (Phase II). Technical report, Organisation for Economic Co-Operation and Development, Nuclear Energy Agency-OECD/NEA, Le Seine Saint-Germain, 12 boulevard des Iles, F-92130 Issy-les-Moulineaux (France), 2013.

[10] D. B. Spalding. A single formula for the ”law of the wall”. *Journal of Applied Mechanics*, 28(3):455–458, 1961.

[11] C. Jayatilleke. The influence of Prandtl number and surface roughness on the resistance of the laminar sublayer to momentum and heat transfer. *Prog. Heat Mass Transfer*, 1:193–321, 1969.

[12] F. R. Menter and T. Esch. Elements of Industrial Heat Transfer Prediction. 16th Brazilian Congress of Mechanical Engineering (COBEM), 2001.

[13] W. G. Luscher and K. J. Geelhood. Material property correlations: Comparisons between FRAPCON-3.4, FRAPTRAN 1.4, and MATPRO. Technical Report NUREG-CR-7024, Pacific Northwest National Laboratory, 2011.